

Chandra Multiwavelength Project (ChaMP) X-ray Point Source Number Count Relations

Minsun Kim, Dong-Woo Kim, Wayne A. Barkhouse, Nancy R. Evans, Paul J. Green, Eunhyeuk Kim, Myung-Gyoon Lee, Amy E. Mossman, John D. Silverman, Harvey D. Tananbaum, Belinda J. Wilkes, and ChaMP collaboration

Harvard-Smithsonian Center for Astrophysics, Smithsonian Astrophysical Observatory
60 Garden Street, Cambridge, MA, USA, mki@cfa.harvard.edu



ABSTRACT

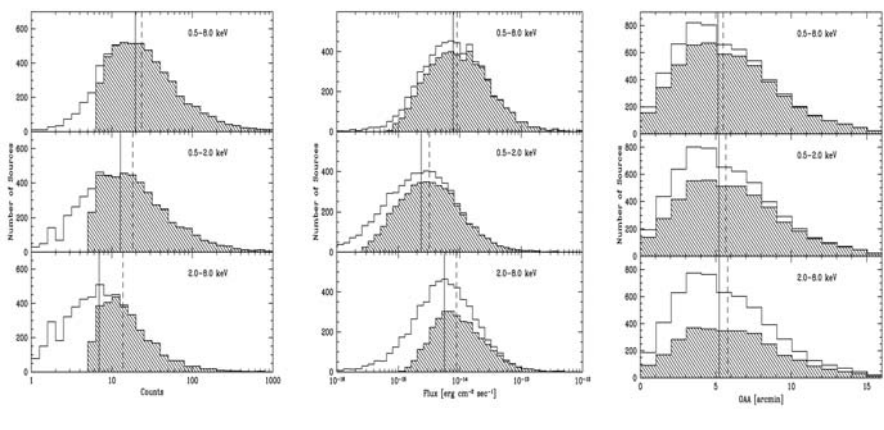
We present the Chandra Multiwavelength Project (ChaMP) X-ray point source number count relations. From the ChaMP X-ray point source catalog, ~4,500, ~3,000, and ~5,500 X-ray point sources are selected to derive the number count relations in the soft, hard, and broad bands, respectively. The full sky coverage area of selected sources is ~9.3 deg². To characterize the sensitivity and completeness as a function of flux, off-axis angle, and background level, we performed a large set of simulations. We generated ~13,000 artificial X-ray sources per deg², added them to each Chandra observation in the ChaMP sample and run the same procedures of detection and source extraction as in the ChaMP data processing.

Number count relations are fitted by a broken power law in differential number count space and compared with number counts relations in Chandra deep fields and other surveys. Also, we simultaneously fitted the ChaMP number count relations and Chandra deep fields. These number count relations cover very large flux ranges, $f_{0.5-2.0} = 3 \times 10^{-17} - 10^{-12}$ and $f_{2.0-8.0} = 2 \times 10^{-16} - 10^{-11}$ in cgs units, with the smallest statistical errors yet reported in any survey.

I. CHAMP DATA

The full X-ray point source catalogue of ChaMP includes ~6,800 X-ray sources of 149 Chandra fields. We selected 130 out of 149 ChaMP fields excluding 19 multi-observed fields. To construct the ChaMP X-ray point source number counts relations, the sources in the 10, 11, 12, and 13 CCD chips for ACIS-I, and in the 12, 13, S2, and S3 CCD chips for ACIS-S of the main ChaMP X-ray point source catalog were selected.

The number distributions of selected X-ray point sources as a function of count, flux, and off axis-angle, in the broad, soft, and hard bands are displayed in following figures. The solid histograms are number distributions of all sources in each band and the shade histograms are the number distributions of sources having S/R > 1.5. Solid and dashed vertical lines represent median values of solid and shaded histograms, respectively.



II. CHAMP SIMULATIONS

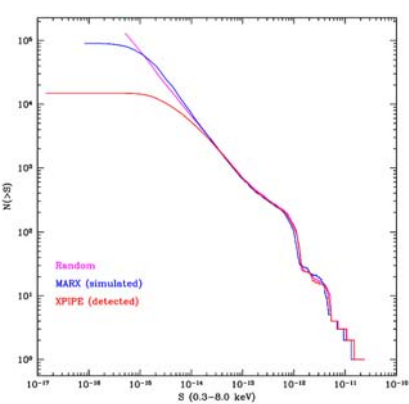
To characterize the sensitivity, completeness, and sky coverage area of ChaMP fields, we have performed a series of simulations. Eddington bias, that the sources with counts near the detection threshold will be preferentially detected when they have upward fluctuations, is also corrected. These biases affect the result considerably at the fainter end of Log(N)-Log(S).

Simulation Process

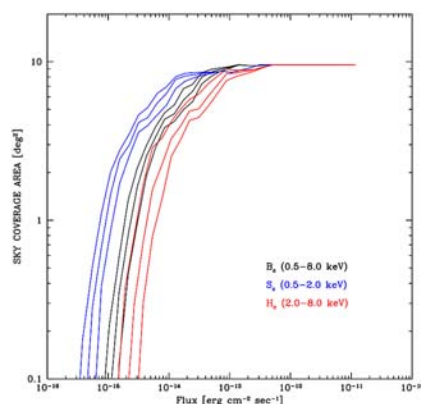
1. Generate artificial X-ray sources with MARX (<http://space.mit.edu/CXC/MARX>)
2. Add artificial X-ray sources to the real observed image.
3. Detect artificial X-ray sources with *wavdetect* (<http://cxc.harvard.edu/ciao>).
4. Extract artificial X-ray source properties with *xapphot* (Kim, E. in preparation)
5. Compare input and output artificial X-ray source properties

Assumptions and Ingredients

1. Power law number counts distribution with a slope of -1
2. Power law energy distribution with Γ_{ph} and the Galactic absorption N_H
3. ~13,000 artificial X-ray sources per deg²
4. Randomly selected the flux from (1) in range of $f = 5 \times 10^{-16} - 5 \times 10^{-10}$ [erg cm⁻² sec⁻¹] in B band, and randomly selected positions of artificial X-ray sources



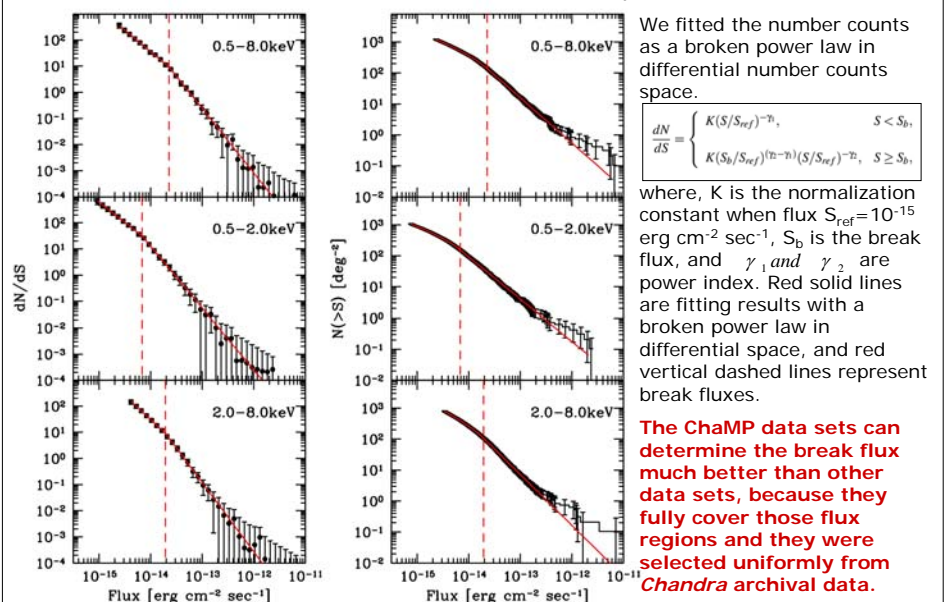
The broad-band cumulative Log(N)-Log(S) relation of the artificial X-ray sources in the 130 Chandra observations. The purple, blue, and red histograms represent the Log(N)-Log(S) relations, that of randomly selected, simulated, and detected artificial X-ray sources.



The sky coverage area of the artificial X-ray sources in B, S, and H bands of the 130 ChaMP fields. The full sky coverage area for these fields is ~9.3 deg². The sky coverage areas for the sources having signal to noise ratios of SNR > 1.5, 2.0, and 2.5 are shown in each energy band, respectively.

III. X-RAY POINT SOURCE NUMBER COUNTS

Following figures show the ChaMP X-ray point source Log(N)-Log(S) relations in broad (*top*), soft (*middle*), and hard (*bottom*), respectively. Differential and cumulative Log(N)-Log(S) relations are displayed in left and right panels, respectively. $\Gamma_{ph} = 1.4$ are assumed.



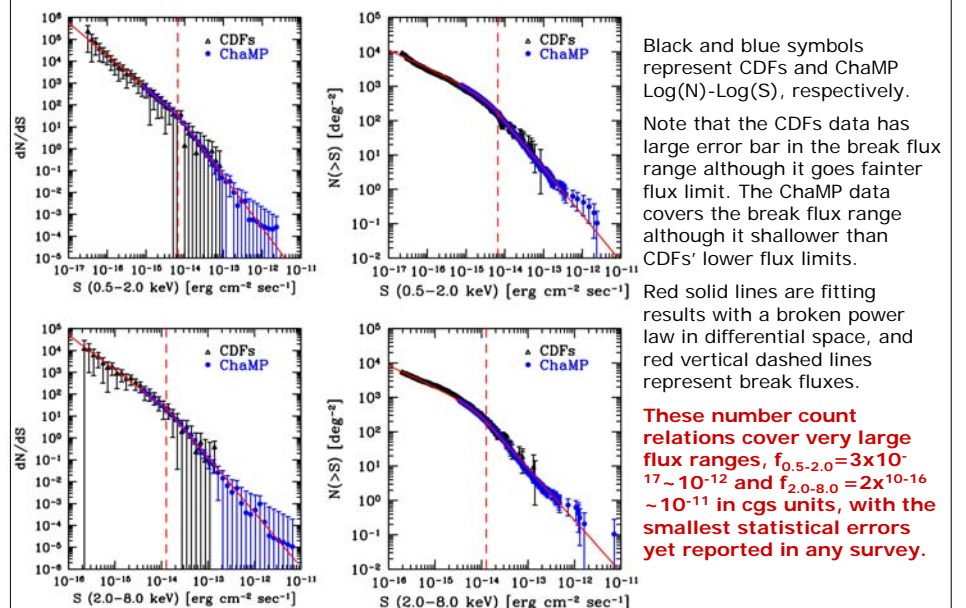
We fitted the number counts as a broken power law in differential number counts space.

$$\frac{dN}{dS} = \begin{cases} K(S/S_{br})^{-\gamma_1}, & S < S_{br} \\ K(S/S_{br})^{-(\gamma_1-\gamma_2)}(S/S_{br})^{-\gamma_2}, & S \geq S_{br} \end{cases}$$

where, K is the normalization constant when flux $S_{br} = 10^{-15}$ erg cm⁻² sec⁻¹, S_{br} is the break flux, and γ_1 and γ_2 are power index. Red solid lines are fitting results with a broken power law in differential space, and red vertical dashed lines represent break fluxes.

The ChaMP data sets can determine the break flux much better than other data sets, because they fully cover those flux regions and they were selected uniformly from Chandra archival data.

Also, we simultaneously fitted the ChaMP Log(N)-Log(S) and CDFs Log(N)-Log(S) (Bauer et al., 2004, AJ, 128, 2048) in differential space. Results are shown in following figures.



Black and blue symbols represent CDFs and ChaMP Log(N)-Log(S), respectively.

Note that the CDFs data has large error bar in the break flux range although it goes fainter flux limit. The ChaMP data covers the break flux range although it shallower than CDFs' lower flux limits.

Red solid lines are fitting results with a broken power law in differential space, and red vertical dashed lines represent break fluxes.

These number count relations cover very large flux ranges, $f_{0.5-2.0} = 3 \times 10^{-17} - 10^{-12}$ and $f_{2.0-8.0} = 2 \times 10^{-16} - 10^{-11}$ in cgs units, with the smallest statistical errors yet reported in any survey.

IV. COMPARISON WITH OTHER STUDIES

Table 4. List of Fitting Parameters of Other Studies and ChaMP

Data	Band	Γ_{ph}	Number	K	γ_1	γ_2	S_{br}	Fit ^a	Reference
(1)	(2)	(3)	(4)	(5)	(6)	(7)	(8)	(9)	(10)
SSA13	0.5-2	1.4	22	722	0.7 ± 0.2	—	—	C.S.	Moshirsky et al. (2000)
	2-10	1.2	15	3949	1.05 ± 0.35	—	—	C.S.	Moshirsky et al. (2000)
CDF-S	2-8	1.2	373	—	1.63 ± 0.05	2.57 ± 0.22	12	D.B.	Covino et al. (2002)
SSA13	0.5-2	1.4	—	490 ± 90	1.53 ± 0.10	—	—	D.B.	Rosati et al. (2002)
	2-10	1.4	—	1500 ± 100	1.61 ± 0.10	—	—	D.B.	Rosati et al. (2002)
	5-10	1.4	—	1230 ± 200	1.18 ± 0.20	—	—	D.B.	Rosati et al. (2002)
CDF-S	0.5-2	1.4	346	380 ± 80	1.63 ± 0.13	—	~13	D.B.	Rosati et al. (2002)
	2-10	1.4	251	1300 ± 100	1.61 ± 0.10	—	~8	D.B.	Rosati et al. (2002)
	5-10	1.4	110	940 ± 100	1.35 ± 0.15	—	—	D.B.	Rosati et al. (2002)
SEXTI	2-10	—	~46.8 ± 2.1	1.41 ± 0.17	2.46 ± 0.08	~12.5	D.D.	Harrison et al. (2003)	
BMW ^b	0.5-2	1.4	4786	6150 ⁺¹⁰⁰⁰	0.60 ^{+0.07}	1.82 ^{+0.09}	14.8 ^{+1.2}	C	Moretti et al. (2003)
ASC ^c	2-10	1.4	1026	5300 ⁺¹⁰⁰⁰	0.44 ^{+0.11}	1.57 ^{+0.08}	4.5 ^{+1.1}	C	Moretti et al. (2003)
CDF-N ^a	0.5-2	1.4	724	3039 ⁺¹⁰⁰	0.55 ± 0.03	—	—	C	Bauer et al. (2004)
	2-8	1.4	520	7403 ⁺¹⁰⁰	0.56 ± 0.14	—	—	C	Bauer et al. (2004)
ChaMP	0.5-2	1.7	707	2030 ± 210	1.40 ± 0.30	2.2 ± 0.30	6 ± 2	D.B.	Kim et al. (2004b)
	2-8	1.4	236	3160 ± 250	—	2.10 ± 0.10	—	C.S.	Kim et al. (2004b)
CLASS	0.5-2	1.4	310	12.69 ± 0.02	1.7 ± 0.2	2.5/(flow)	10	D.D.	Yang et al. (2004)
	2-8	1.4	235	45.60 ± 0.5	1.65 ± 0.4	2.4 ± 0.6	—	D.D.	Yang et al. (2004)
XMM-LSS	0.5-2	1.7	1028	384.2	1.42 ^{+0.14}	2.62 ^{+0.22}	10.6 ^{+2.2}	D.B.	Chappetti et al. (2005)
	2-10	1.7	328	4.5 × 10 ⁴	1.53 ^{+0.11}	2.91 ^{+0.21}	21.4 ^{+5.1}	D.B.	Chappetti et al. (2005)
ChaMP	0.5-2	1.4	4554	612.12 ^{+12.11}	1.55 ^{+0.11}	2.36 ^{+0.10}	6.30 ^{+1.52}	D.B.	this study
	2-8	1.4	3078	2066.30 ^{+10.21}	1.83 ^{+0.11}	2.66 ^{+0.10}	19.39 ^{+3.52}	D.B.	this study
	0.5-8	1.4	5229	1561.83 ^{+10.85}	1.64 ^{+0.11}	2.46 ^{+0.11}	22.70 ^{+3.76}	D.B.	this study
	0.3-2.5	1.4	4864	995.17 ^{+11.27}	1.76 ^{+0.11}	2.43 ^{+0.11}	7.42 ^{+1.01}	D.B.	this study
	2.5-8	1.4	2875	1645.60 ^{+105.02}	1.76 ^{+0.20}	2.55 ^{+0.11}	15.79 ^{+1.81}	D.B.	this study
	0.3-8	1.4	5515	1645.60 ^{+105.02}	1.65 ^{+0.20}	2.43 ^{+0.11}	25.43 ^{+3.45}	D.B.	this study
ChaMP ^a	0.5-2	1.4	4554 + 724	576.17 ^{+10.21}	1.50 ^{+0.11}	2.36 ^{+0.11}	6.63 ^{+1.52}	D.B.	this study
	2-8	1.4	3078 + 520	1310.76 ^{+11.46}	1.59 ^{+0.11}	2.51 ^{+0.11}	12.62 ^{+1.81}	D.B.	this study

Best fitting parameters of the ChaMP and other survey X-ray point source number counts are listed in Table 4.

The ChaMP results agree well with other studies (1σ) but present parameters with the smallest statistical errors. The ChaMP data sets can determine the break flux much better than other data sets.

^aNormalized with 10^{-15} in cgs units

^bC for cumulative and D for differential fitting space. S for a single power law and B for a broken power fitting.

V. CONCLUSION

We present the ChaMP logN-logS relations in multiple X-ray energy bands. We have used ~5,500 X-ray sources detected from 130 ChaMP fields covering ~9.3 deg² in sky area. To correct the incompleteness and to determine sky coverage area, we have performed extensive simulations. The number count relations are fitted by a broken power law in differential number count space and fitting results agree with previous studies in 1σ error range. We also present the simultaneous fitting results of ChaMP and CDFs data. These number count relations cover very large flux ranges, $f_{0.5-2.0} = 3 \times 10^{-17} - 10^{-12}$ and $f_{2.0-8.0} = 2 \times 10^{-16} - 10^{-11}$ in cgs units, with the smallest statistical errors yet reported in any survey, serving as strong constraints on population and evolution models of cosmic X-ray sources.